Influence of the Arctic Oscillation and El Niño-Southern Oscillation (ENSO) on ice conditions in the Baltic Sea: The wavelet approach

S. Jevrejeva

Proudman Oceanographic Laboratory, Birkenhead, UK

J. C. Moore and A. Grinsted

Arctic Centre, University of Lapland, Rovaniemi, Finland

[1]   Variability in time series of ice conditions in the Baltic Sea is examined within the context of atmospheric circulation represented by the North Atlantic Oscillation (NAO) and Arctic Oscillation (AO) winter indices using the wavelet approach. We develop methods of assessing statistical significance and confidence intervals of cross-wavelet phase and wavelet coherence. Cross-wavelet power for the time series indicates that the times of largest variance in ice conditions are in excellent agreement with significant power in the AO at 2.2–3.5, 5.7–7.8, and 12–20 year periods, similar patterns are also seen with the Southern Oscillation Index (SOI) and Niño3 sea surface temperature (Niño3) series. Wavelet coherence shows in-phase linkages between the 2.2–7.8 and 12–20 year period signals in both tropical and Arctic atmospheric circulation and also with ice conditions in the Baltic Sea. These results are consistent with GCM simulations showing dynamical connections between high-latitude surface conditions, tropical sea surface temperatures mediated by tropical wave propagation, the wintertime polar vortex, and the AO and with models of sea ice and oceanic feedbacks at decadal periods.   *INDEX TERMS:* 1620 Global Change: Climate dynamics (3309); 3337 Meteorology and Atmospheric Dynamics: Numerical modeling and data assimilation; 3339 Meteorology and Atmospheric Dynamics: Ocean/atmosphere interactions (0312, 4504); 4522 Oceanography: Physical: El Niño; 9345 Information Related to Geographic Region: Large bodies of water (e.g., lakes and inland seas); *KEYWORDS:* wavelet, MC-SSA, AO, NAO, ENSO, Baltic Sea ice conditions

1.   Introduction

[2]   The El Niño-Southern Oscillation (ENSO) and the Northern and Southern Annular Modes are the largest climate fluctuations on the planet. The Northern Annular Mode is usually referred to as the Arctic Oscillation (AO) [*Thompson and Wallace*, 1998], and naturally has a great influence on general Arctic climate [e.g., *Moritz et al.*, 2002]. While both ENSO and AO phenomena have received extensive treatment over the past decade and earlier, the possible connection between them that is sometimes shown in GCM models [*Hoerling et al.*, 2001; *Merkel and Latif*, 2002], has fairly limited supporting observational evidence [*Baldwin and Dunkerton*, 2001; *Dong et al.*, 2000]. Studies indicate that the impacts of ENSO are more readily seen in the north Atlantic sector during winter than summer, that there is a roughly 3-month lag between tropical signal and extra-tropical response, and that signal-to-noise ratio is rather low [*Trenberth*, 1997; *Pozo-Vázquez et al.*, 2001; *Cassou and Terray*, 2001]. These considera-

tions motivate our approach in developing novel wavelet approaches and applying them to simultaneously extract both the signals in noisy datasets, and the phase angle between tropical and North Atlantic/Arctic signals.

[3]   The Baltic Sea is a transition zone between the North Atlantic region and the continental area of Eurasia, which is the main reason for the large interannual variability of the ice conditions. The Baltic Sea is partly covered by ice every winter season, the maximum annual ice extent is 10–100 percent of the sea area, the length of ice season is 4–7 months, and the maximum annual thickness of ice is 50–120 cm [*Leppäranta and Seinä*, 1985; *Seinä and Palosuo*, 1996; *Jevrejeva*, 2001; *Seinä et al.*, 2001]. Results published recently demonstrate that large-scale atmospheric circulation patterns in the Arctic and North Atlantic described by the AO or by the somewhat similar North Atlantic Oscillation (NAO) teleconnections significantly control ice conditions in the Baltic Sea [*Koslowski and Glaser*, 1995; *Loewe and Koslowski*, 1998; *Koslowski and Glaser*, 1999; *Omstedt and Chen*, 2001; *Jevrejeva and Moore*, 2001; *Jevrejeva*, 2002]. While there are many similarities between the AO and the NAO (Figure 1a), there has also been a wealth of recent work that shows
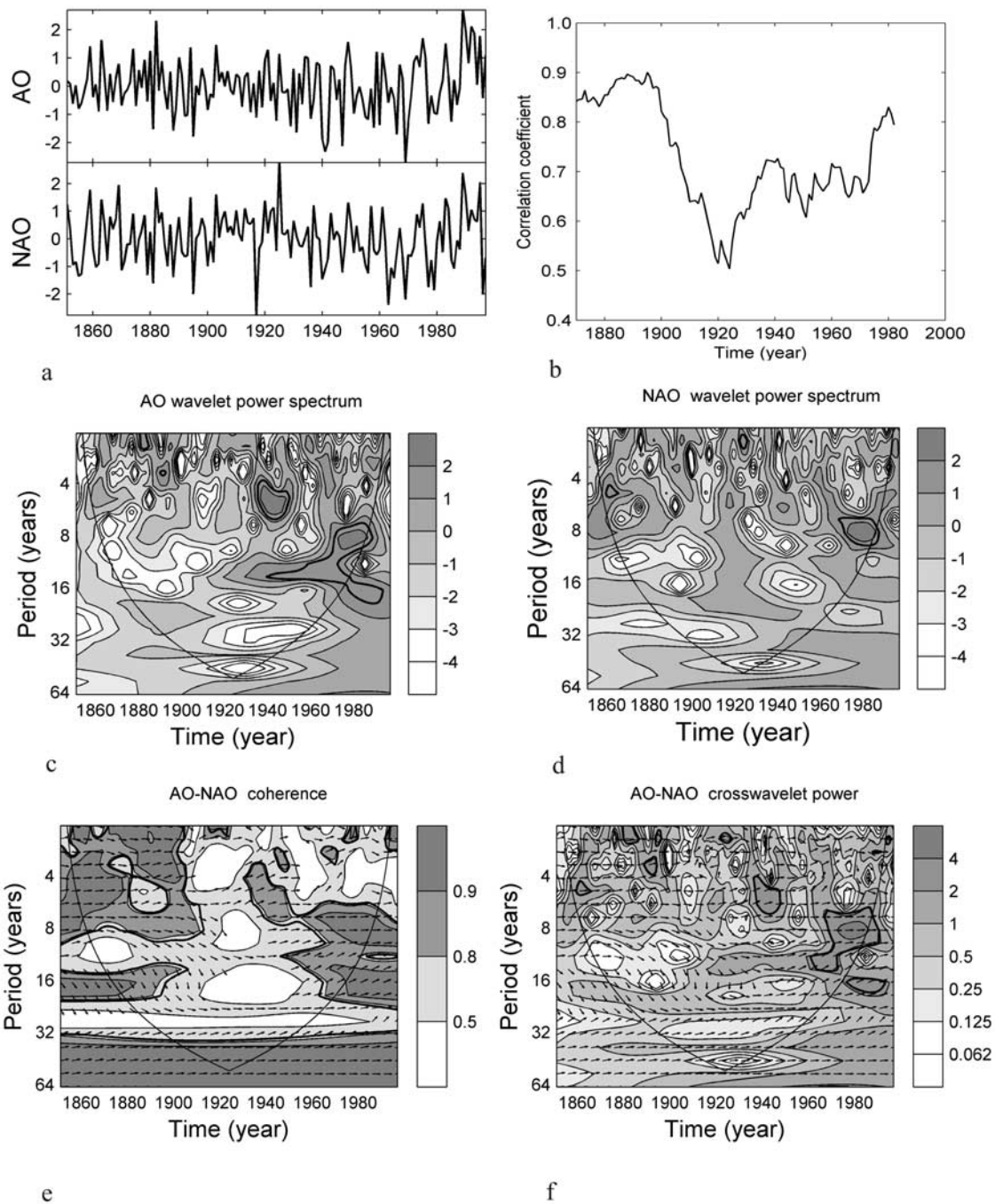
Figure 1. (a) Normalized time series of AO winter index and NAO winter index. (b) Running correlation coefficient between the AO winter index and NAO winter index (30 year window). (c) Wavelet power spectrum (Morlet wavelet) of the AO winter index. (d) The same as Figure 1c but for NAO. (e) The wavelet coherency and phase between AO and NAO. Contours are wavelet squared coherencies. The vectors indicate the phase difference between the AO and NAO (a horizontal arrow pointing from left to right signifies in phase and an arrow pointing vertically upward means the second series lags the first by 90° (i.e., the phase angle is 270°)). (f) The cross-wavelet power between the AO and NAO. Contours are variance units, vectors indicate the phase difference between the AO and NAO. In Figures 1c–1f the thick black line is the 5% significance level using the red noise model, and the thin black line indicates the cone of influence. See color version of this figure in the HTML.

them to be significantly different in both their dynamical interpretation, and their spatial and temporal variability [e.g., *Wanner et al.*, 2001; *Jevrejeva and Moore*, 2001; *Lin et al*, 2002]. The influence of the NAO and the AO on the ice in the Baltic region is not stationary over time. For example, the moving correlation coefficient between the maximum annual ice extent in the Baltic Sea (BMI) and the NAO winter index varies between 0.3 and 0.7

[Omstedt and Chen, 2001] for the period 1865–1995; and the moving correlation coefficients between time series of date of ice break-up, sum of negative degree-days, duration of ice seasons and the NAO winter index shows similar results [Jevrejeva, 2002]. The relationship between the AO and the NAO indices is also not stationary over time (Figure 1b). Jevrejeva and Moore [2001] show that the AO appears to describe more of the dynamics of the Baltic Sea ice conditions than the NAO. In a previous study [Jevrejeva and Moore, 2001] the ENSO quasi-biennial and quasi-quadrennial signals were detected by Monte Carlo Singular Spectrum Analysis (MC-SSA) in time series of the AO, NAO, ice conditions and winter sea surface temperature (SST), which are consistent with results obtained for the time series of sea ice cover from the Arctic and Antarctic [Gloersen, 1995; Venegas and Mysak, 2000] and for the Baltic Sea [Loewe and Koslowski, 1998]. However, the variation over time of amplitude and relative phases of the quasiperiodic signals seen in the times series has not been investigated in any detail, though this is clearly needed to aid identification of forcing mechanisms. We investigate both relationships between the tropical and Arctic/North Atlantic circulation indices, and between ice conditions and polar and tropical circulation patterns.

[4] The objectives of this paper are to elucidate the variability of the ice conditions/atmospheric circulation relationship. We will do this mainly using the wavelet transform (WT) approach, with comparisons to results from MC-SSA. We develop a method of dealing with wavelet analysis of very non-Gaussian distributed data such as the time series of ice conditions in the Baltic Sea. To study the relationships between two time series, we use the wavelet coherence method, introducing a technique of generating confidence intervals for phases against red-noise models. The consistency of the results obtained by the powerful and independent WT and MC-SSA methods should strengthen their credibility. We will give descriptions of the changes in covariance between time series of ice conditions and atmospheric circulation during the last 150 years. We will show that there is significant dependence of the AO and ice conditions on the strength and type of variability of the SOI and Niño3 indices of tropical ocean climate by providing the cross-wavelet power and coherence for the time series. Finally, we address the mechanisms of ice variability in terms of large-scale atmospheric, sea ice and oceanic oscillations.

2. Data

[5] Ice conditions are represented by the time series of maximum annual ice extent in the Baltic Sea (BMI) for the period 1825–2000 [Seinä and Palosuo, 1996; Seinä et al., 2001]. Additionally the date of ice break-up at Riga since 1825 [Jevrejeva, 2001], and at several other Baltic ports, spanning more than 100 years, were analyzed to increase confidence in our findings, but as results are very similar they are not shown here. We discuss winter surface air temperature (SAT) from Uppsala (1825–2000) [Bergström and Moberg, 2002], with some additional results for Stockholm (1825–2000) [Moberg et al., 2002] and St. Petersburg (1825–1996) [Jones and Lister, 2002]. We also examined the calculated sum of negative degree-days, defined as

accumulated negative air temperature during the winter season [Jevrejeva, 2001], for St. Petersburg (1851–1995), Riga (1851–1990) and other Baltic ports, spanning more than 150 years, as another measure of severity of winter seasons [Jevrejeva, 2001]. We do this mainly to strengthen confidence in our assessment of the cross-wavelet power and coherence significance levels for the non-Gaussian BMI time series.

[6] Atmospheric circulation patterns are represented by the NAO winter index (1825–1999), produced by Jones et al. [1997] which is longer than the Hurrell [1995] NAO index and the AO winter data (1851–1997) based on the expansion coefficient time series of the pattern of SAT anomalies associated with the AO [Thompson and Wallace, 1998]. We utilized the same time series as in previous study [Jevrejeva and Moore, 2001] in order to compare the results from WT to the results from MC-SSA.

[7] As the atmospheric component of ENSO, we used the Southern Oscillation index (SOI), for October–December (1866–2001) defined as the normalized pressure difference between Tahiti and Darwin [Ropelewski and Jones, 1987]. We also discuss the oceanic component of ENSO parameterized by the Niño3 SST index during autumn (1857–2001) [Kaplan et al., 1998]. The 3 month lag between the time series of SOI/Niño3 and NAO/AO was found to give the most significant results in our own analysis, and it also is consistent with results from Trenberth and Hurrell [1994], showing a lag of around 3 months between the beginning of ENSO event and the extratropical response in higher latitudes in the North Pacific area; and also with results from Pozo-Vázquez et al. [2001] confirming that there is a similar lag for the North Atlantic region.

3. Methods

[8] We used MC-SSA [Allen and Smith, 1996] to separate nonlinear long-term trends and quasi-regular oscillations from the time series. The key advantage of the method over the conventional Fourier methods is the ability to detect amplitude- and phase-modulated oscillations. A more powerful method for analyzing localized intermittent oscillations is the wavelet transform (WT) [Holschneider, 1995; Foufoula-Georgiou and Kumar, 1995]. Important aspects of nonlinear oscillations in a complex system with multiple timescales, like the climate system, are their modulation in amplitude, phase and frequency. MC-SSA can follow well, via reconstructed components, variations in signal amplitude and phase that are associated with fairly broad spectral peaks. Wavelet analysis provides an even more natural way of following quasi-adiabatic or gradual changes in the natural frequency of a climatic oscillator [Meyers et al., 1993; Yiou et al., 2000]. The bandwidth of the data should be narrow for the WT method to reliably identify them. The method we use to reduce the bandwidth is to normalize the probability density function (pdf) of the data before applying the WT.

3.1. Data Normalization

[9] The maximum extent of the Baltic Sea ice is characterized by a bi-modal probability density function with maximum likelihoods near 0 and 100% ice covered. We would like all the climatic indices and proxies (data) we are

comparing to have the same pdfs. Thus before we do any comparisons we transform the original data using a data adaptive transformation function N.

$$d_{norm} = N(d_{orig}),$$

where d_{orig} is the original data, d_{norm} is the transformed data and N is a monotonically increasing function. The transformation operator N is optimally chosen so that the pdf of d_{norm} is Normal, has zero mean and unit variance. $N(d_i)$ is calculated by making the inverse normal cdf of the percentile which d_i has in the cdf of d. The transformation N is called normalizing. All the wavelet results in this paper are for the normalized time series; in contrast the MC-SSA processing was done on the original time series [see also *Jevrejeva and Moore*, 2001].

[10] Consistency in the results shows that the two methods are complimentary and gives confidence in the results and in the validity of the normalization procedure.

3.2. Wavelet Transforms

[11] The wavelet transform can be used to analyze time series that contain nonstationary power at many different frequencies [*Foufoula-Georgiou and Kumar*, 1995]. The continuous wavelet transform (CWT) of time series is its convolution with the local basis functions, or wavelets, which can be stretched and translated with flexible resolution in both frequency and time. The CWT of the time series d with respect to the wavelet ψ is defined as

$$W_{d,\psi}(s,t) = (d(t) * \psi_s(t)),$$

where t is time and ψ_s is the wavelet at the scale s (which is linearly related to the characteristic period of the wavelet). The wavelet power is defined as $|W_{d,\psi}|^2$. The data $d(t)$ is bounded in time so the wavelet transform is affected by edge effects. Following *Torrence and Compo* [1998], we call this the cone of influence (COI). The CWT decomposes the time series into time-frequency space, enabling the identification of both the dominant modes of variability and how those modes vary with time. In this paper, we use the Morlet wavelet as it is quite well localized in both time and frequency space, other wavelet bases, such as Paul, were also tested in order to obtain better time localization, and gave essentially the same results. Statistical significance was estimated [*Torrence and Compo*, 1998] against a red noise model.

[12] For analysis of the covariance of two time series we follow *Torrence and Compo* [1998] and define the cross-wavelet spectrum of two time series X and Y with wavelet transforms W_X and W_Y as

$$W_{XY}(s,t) = W_X(s,t)W_Y^*(s,t),$$

where asterisk denotes complex conjugation. Further we define the cross-wavelet power $|W_{XY}(s,t)|$. The phase angle of W_{XY} describes the phase relationship between X and Y in time-frequency space. Statistical significance is estimated against a red noise model [*Torrence and Compo*, 1998].

[13] As we are interested in the phase difference between the components of the two time series we need to estimate the mean and confidence interval of the phase difference. We used the circular mean of the phase for those regions with higher than 5% statistical significance and which are outside the COI to quantify the phase relationship. We calculate the 95% confidence angle of the mean phase assuming a Von Mises distribution [e.g., *Zar*, 1999]. The spread of the Von Mises distribution is characterized by a parameter, κ, which characterizes the local phase field with respect to its information quality. For small κ the phases tend to a uniform distribution and for large κ they tend to a normal distribution with variance $1/\kappa$. This is a useful and general method for calculating the significance of phase angles for the time series used.

[14] Another useful tool is the wavelet coherence. Coherence is a measure of the intensity of the covariance of the two series in time-frequency space, unlike the cross-wavelet power which is a measure of the common power. Again, beginning with the approach of *Torrence and Webster* [1999], we define the coherence as

$$R^2(s,t) = \frac{|S(s^{-1}W_{XY}(s,t))|^2}{S\left(s^{-1}|W_X(s,t)|^2\right) \cdot S\left(s^{-1}|W_Y(s,t)|^2\right)},$$

where S is a smoothing operator. The scales in time and frequency over which S is smoothing define the scales at which the coherence measures the covariance. We write the smoothing operator S as

$$S(W) = S_{scale}(S_{time}(W(s,t))),$$

where S_{scale} denotes smoothing along the wavelet scale axis and S_{time} smoothing in time. The natural way to design the smoothing operator for the Morlet wavelet is given by *Torrence and Webster* [1998]

$$S_{time}(W)|_s = \left(W(t,s) * c_1 e^{-t^2/2s^2}\right)\Big|_s,$$

$$S_{scale}(W)|_t = (W(t,s) * c_2 \Pi(0.6s))|_t$$

where c_1 and c_2 are normalization constants and Π is the rectangle function. The factor of 0.6 is the empirically determined scale decorrelation length for the Morlet wavelet [*Torrence and Compo*, 1998].

[15] *Torrence and Webster* [1999] estimated coherence significance levels against only a white noise model, but here we use Monte Carlo methods with red noise to determine the 5% statistical significance level of the coherence. Empirical testing indicates that the color of the noise (determined by the first order autoregressive coefficients of the two original time series) has no influence on the magnitude of the coherence corresponding to the 5% significance level, whereas the specifics of the smoothing operator have a large influence. Further the 5% statistical significance level of the coherence seems to be constant (≈ 0.78) across all scales except where S_{scale} is influenced by domain boundaries.

[16] The difference between the phase angles determined by the cross-wavelet and coherence methods is essentially

only the smoothing used in the coherence method. Therefore, for simplicity, we only quote the phase angles and the confidence intervals determined for the coherence analysis. In this paper we give the mean phase and its 95% confidence interval as its error.

4. Results

4.1. NAO and AO Winter Index

[17] The distinction between the NAO and the AO is discussed in many papers, and interpretation of the NAO and the AO is currently open to debate [*Deser*, 2000; *Wallace*, 2000; *Ambaum et al.*, 2001; *Lin et al.*, 2002]. *Thompson and Wallace* [1998] assumed that the AO includes a smaller scale oscillation already recognized as the reigning climate maker in the North Atlantic region- the NAO. According to *Deser* [2000], there is no coordinated behavior of the Atlantic and the Pacific center of action and the annular appearance of the AO is determined by the Arctic center of action. The NAO reflects the correlation between the surface pressure variability at all of its centers of action whereas this is not the case for the AO [*Ambaum et al.*, 2001]. Time series of normalized NAO and AO winter indices provide evidence for dissimilar variability in the two time series (Figure 1a). The Pearson correlation coefficient between the NAO and AO winter indices for the period 1851–1997 is 0.7; however, the relationship is not stable over time. Figure 1b shows the running correlation coefficient between NAO and AO as a function of date. Values are around 0.8–0.9 for the period prior to 1900 and the last 30 years, but there are several periods with much lower values, the most notable being a broad minimum between 1905–1930. The high correlations for the period prior 1900 may be explained by deficiencies in the reconstructed data - no direct measurements of SLP in the Arctic are used. We examine the NAO/AO relationship further by decomposing the time series of NAO and AO winter indices in time-frequency space in order to determine both the dominant modes of variability and how those modes vary in time. MC-SSA shows that, in general, NAO and AO consist of the same leading signals with near-identical quasiperiodicity [*Jevrejeva and Moore*, 2001], namely, 2.2–2.4, 7.8, and 12.8 years. Nevertheless there are remarkable differences in how those signals change over time, and also rather dissimilar contributions from those signals to the total variance. The time-frequency patterns (Figures 1c and 1d) are not analogous for the two time series, particularly during 1920–1950. The wavelet coherency between NAO and AO is shown in Figure 1e. The NAO and AO show high coherency in the 2–3.5, 5.2–7.8 and 12–20 year bands, with rather low coherency outside of these periods from 1910 to 1950. Since 1950 there is a shift in the period of maximum coherence from around 2–7.8 years up to around 7.8–20 years. The low coherency of 2–15 year signals through 1920–1935 or 15–30 years during 1910–1960 suggest that independent processes (noise) drive at the smallest and largest scales.

[18] The vectors in Figures 1e and 1f indicate the phase difference between NAO and AO at each time and period. Calculated mean angle and 95% confidence interval of the wavelet coherence are $358° ± 2°$, confirming the rather narrow phase angle distribution. The phase difference in

regions below a wavelet coherence value of 0.8 is more randomly distributed.

[19] The AO exhibits a significant power peak in the 3.5–7.8 year band between 1935–1950, which is also associated with a period of higher power at 3.5–7.8 years in SOI and Niño3 (Figure 2). Cross-wavelet power (Figures 2e and 2f) and coherence (Figures 2c and 2d) indicate large covariance between SOI/AO and Niño3/AO indices at scales of 3.5–7.8 years. Furthermore, the coherence phase is $358° ± 9°$, showing that SOI and AO signals are in phase. The coherence phase between Niño3 (which is 180° out of phase with SOI), and AO is $200° ± 10°$. High power and coherence in the AO associated with signals on the 12–20 year timescales since 1940 is linked to the SOI (Figures 2a, 2c, 2e, and 3).

[20] The cross-wavelet power, coherence and phase difference between time series of SOI/NAO and Niño3/NAO were also calculated but are not shown here. Cross-wavelet power results are very similar to those for SOI/AO and Niño3/AO. Nevertheless, for the NAO, the phase is fairly randomly distributed. The wavelet power spectrum in the 7.8–12.8 year band is very similar for the NAO and AO during 1960–90; those signals with periods of 7.8–12.8 years are associated with variability of SST in North Atlantic Ocean [*Moron et al.*, 1998]. However, the AO shows higher power in the 2.2–5.7 year band for 1960–1970 than the NAO. These features are clearly associated with high power in the same bands in Niño3, confirmed by the cross-wavelet results (Figures 2d and 2f), where the large covariance between the AO and Niño3 is antiphase.

[21] In general, the results demonstrate AO contains tropically forced components represented by the signals in the 2.2–7.8 and 12–20 year bands of the SOI and Niño3.

4.2. Winter SAT

[22] Variability of SAT is contained within the 2–13 year band and not distributed uniformly over time. Time series of SAT (Uppsala, Stockholm, Riga and St. Petersburg) show high power at the 2.2–2.8 year and 3.5–5.7 year timescales over the past 150 years, with high power in the 7.8–12.8 year band only between 1825–1840 and 1960–1990. Results from cross-wavelet analysis between the SAT time series and the NAO and AO winter indices (not shown here) demonstrate the similar high variability during 1880–1900, 1935–1950 and 1960–1990. The 2.2–12.8 year band of SAT and the NAO/AO winter index are consistent and in-phase ($0° ± 2°$) with high cross-wavelet power and coherence. The signature from SOI and Niño3 associated with 2.2–3.5 year signals during 1890–1900, 3.5–7.8 year signals between 1940–50, and 12–20 year signals since 1940 is seen in time series of SAT (Figure 4), where the phase angle in these zones is $0° ± 2°$ For SOI and $180° ± 4°$ For Niño3, suggesting the influence of SOI and Niño3 on SAT variability.

4.3. Ice Conditions Time Series

[23] Baltic Sea ice condition variability during the past 150 years is mainly associated with signals in the 2.2–3.5, 5.7–7.8 and 12.8 year bands.

[24] In general, our results show that the AO is a more complete representation of the driving force during the winter seasons in the Baltic Sea than the NAO. There is a
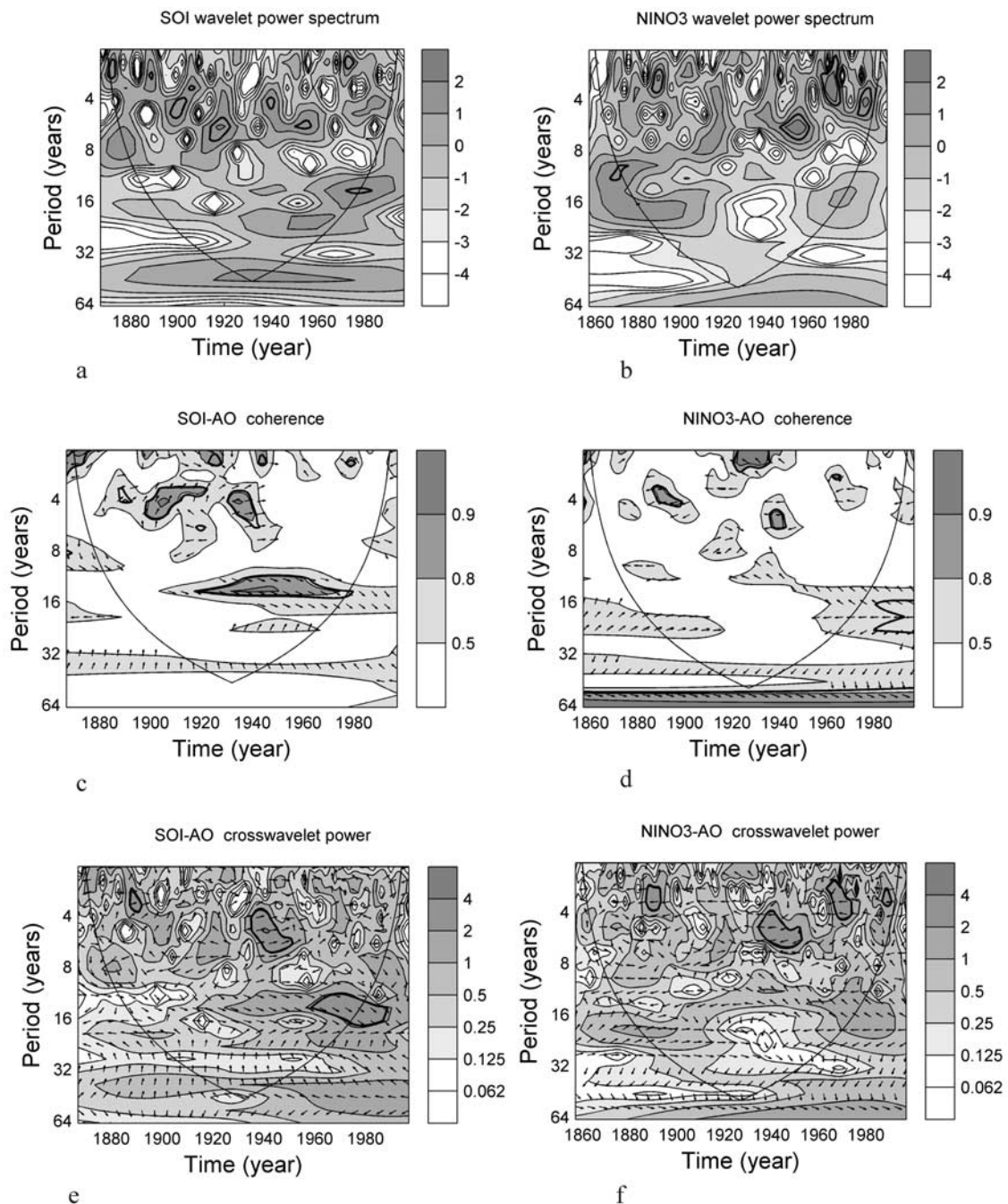
Figure 2. The wavelet power spectrum of (a) SOI index and (b) Niño3 index; the wavelet coherency and phase between (c) SOI and AO and (d) Niño3 and AO. Contours are wavelet squared coherencies, and vectors indicate the phase difference between the SOI/AO (Figure 2c) and Niño3/AO (Figure 2d); the cross-wavelet power between SOI and AO (Figure 2e) and Niño3 and AO (Figure 2f). Contours are for variance units. The vectors indicate the phase difference between the SOI/AO and Niño3/AO. In all panels the thick black line is the 5% significance level using the red noise model, and the thin black line indicates the cone of influence. See color version of this figure in the HTML.

good agreement between the intervals of higher power in the 2.2–2.8 and 3.5–5.7 year bands of the AO winter index and time series of BMI throughout 1880–1900 (Figures 5a and 5c). *Jevrejeva and Moore* [2001] showed with MC-SSA that these signals are related to the quasi- biennial oscillations (QBO) in SOI and Niño3 time series, which is in agreement with results obtained by *Moron et al.* [1998],

confirming WT analysis by other authors of the SOI and Niño3 series [*Torrence and Compo*, 1998; *Torrence and Webster*, 1999; *Yiou et al.*, 2000]. Figure 5 shows a rather stable phase difference (180° ± 2°) between time series of ice conditions and the AO, except for a relatively low covariance interval between 1900 and 1925, accompanied by rather random phase behavior (Figure 5c). As already
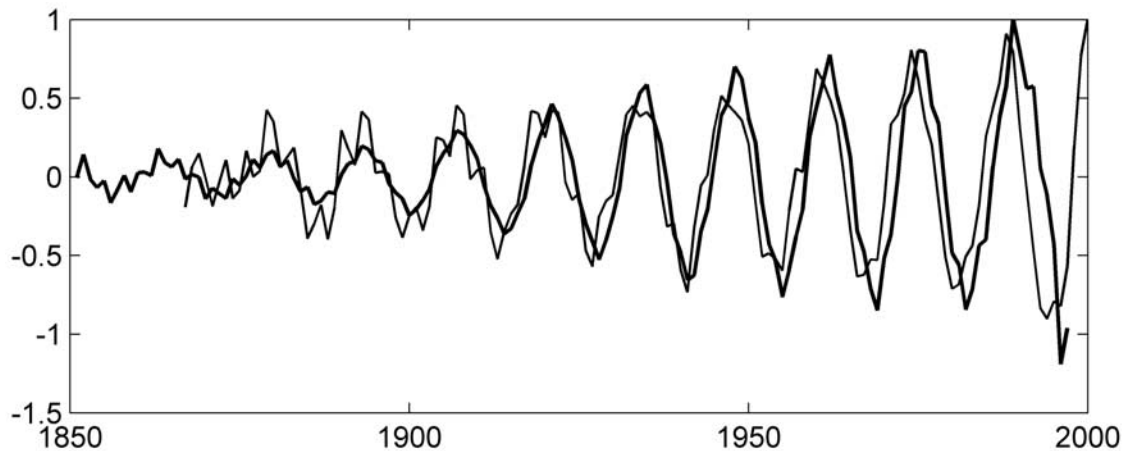
Figure 3. SSA standardized components of the 13.9 year oscillation in winter AO (thick line) and the 13.5 year oscillation in autumn SOI (thin line); results are significant at the 95% level against a white noise model.

mentioned, 1900–1925 is within the period of lowest correlation between the AO and NAO (Figure 1); as well as the period of weakest correlation coefficient between the NAO and BMI [*Omstedt and Chen*, 2001]. The lowest correlation between the NAO index and SAT was detected for the period of 1900–20 [*Chen and Heliström*, 1999].

[25] Between 1935 and 1950 the influence of AO on BMI and time series of sum of negative degree-days in the 3.5–7.8 year band is clearly seen (Figure 5). In comparison, results from cross-wavelet analysis of NAO winter index BMI show similar patterns in cross-wavelet power spectrum; however, the phase is more randomly distributed.

[26] Similar results (not shown here) are also found for the time series of ice break-up at Riga, Helsinki and from some other ports in the northern and central part of the Baltic Sea with those found by *Loewe and Koslowski* [1998] for their accumulated areal ice volume data series for the western Baltic Sea. The small differences in strengths of the various signals found are probably due to local effects in

specific ports, and may be viewed as noise in the regional scale signal we are searching for by using the maximum ice extent series.

[27] The relationship between the Niño3/SOI and ice conditions can also be examined using the time series of sum of negative degree-days from several stations (e.g., St. Petersburg and Riga) situated along the Baltic Sea coast spanning about 150 years, as an alternative measure of ice severity [*Jevrejeva*, 2001]. We did this mainly to confirm our results with respect to the normalization procedure discussed in Section 3. In general, the results are in good agreement with those using the normalized BMI, and again confirm the influence from SOI and Niño3 on severity of winter seasons. Cross-wavelet and coherence are shown in Figure 6. There is significant cross-wavelet power and consistent phase angle for the period 1886–90 associated with signals in the 2.2–3.5 year band, between 1938–1947 with 5.2–7.8 year signals, and 1960–90 with 12–20 year signals; outside of those time periods the phase angle is
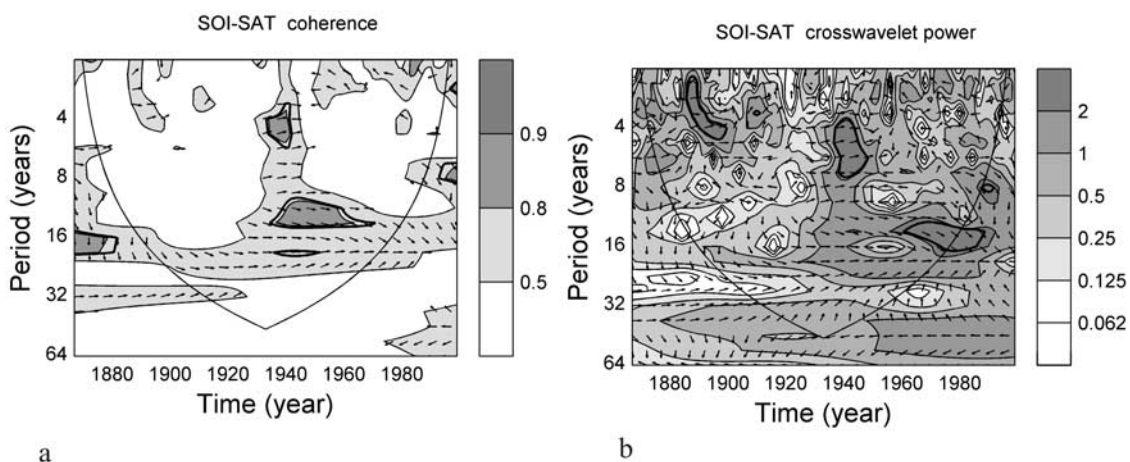

Figure 4. (a) The wavelet coherency and phase between SOI and SAT at Riga. Contours are wavelet squared coherencies. (b) The cross-wavelet power between SOI and SAT. Contours are for variance units. The vectors indicate the phase difference between the SOI/SAT. The thick solid line is the 5% significance level using the red noise model, and the thin solid line indicates the cone of influence.
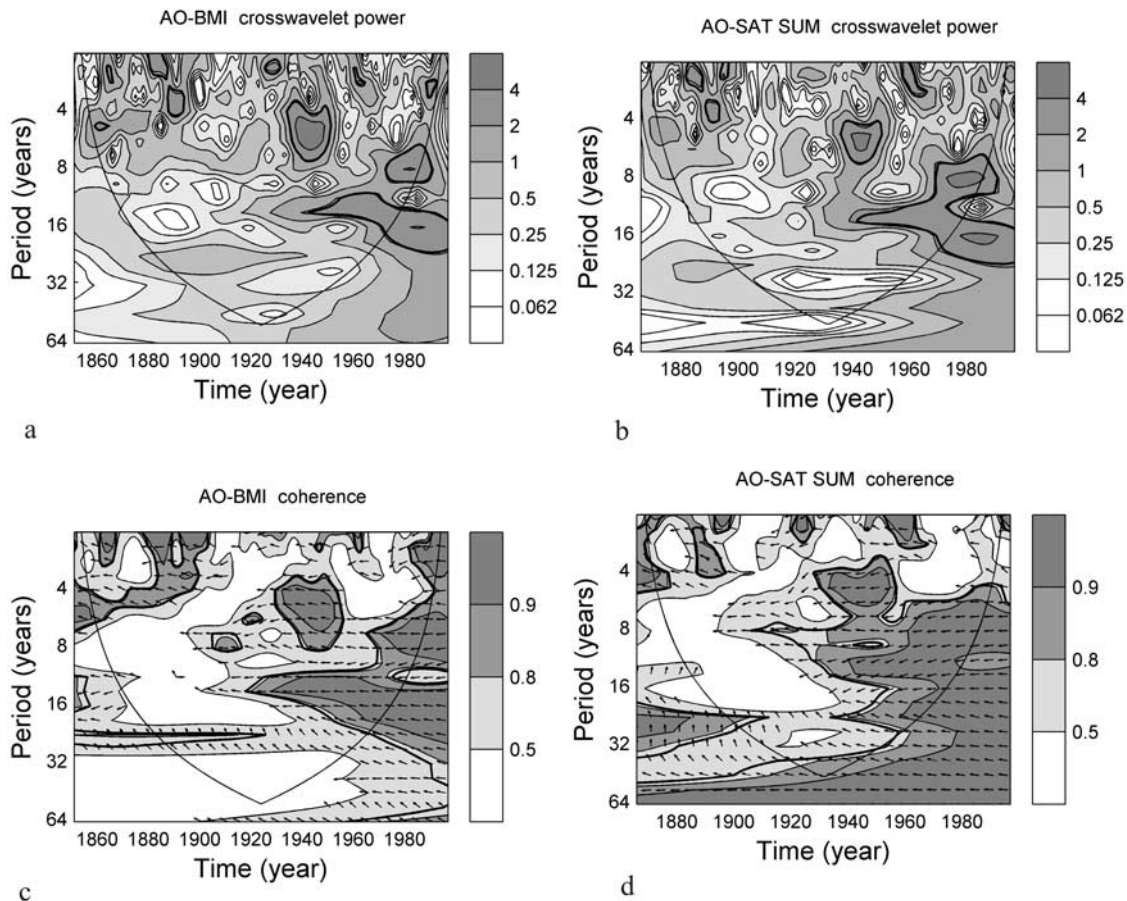
Figure 5. (a) The cross-wavelet power for the AO winter index and BMI and (b) cross-wavelet power for the AO winter index and sum of negative degree days at Riga (SAT SUM). (c) The wavelet coherency and phase between AO and BMI . Contours are wavelet squared coherencies; the vectors indicate the phase difference between the AO and BMI. (d) The same as Figure 5c but for AO and SAT SUM. The thick black line is the 5% significance level using the red noise model, and the thin black line indicates the cone of influence. See color version of this figure in the HTML.

rather chaotic. The 12–20 year oscillations seen in Niño3 and SOI are linked to a 12–20 year amplitude modulation of ENSO events found by *Mak* [1995] and *Torrence and Webster* [1999].

5. Discussion

[28] Our results provide evidence of differences between the NAO and the AO, and of their influence on the ice conditions in the Baltic Sea. We have shown that the AO contains tropically forced components represented by signals in the 2.2–3.5, 5.7–7.8 and 12–20 year bands. The highest variability in ice conditions occurs with the same periodicities and is linked to the AO and with SOI and Niño3 signals. The influence of equatorial Pacific Ocean SST variability is more evident in the AO than the NAO, which is consistent with results from experiments with a simple general circulation model showing the importance of tropical forcing for variability in AO [*Lin et al.*, 2002]. There are traces of the Niño3 and the SOI signals at 2.2–7.8 year periods in cross-wavelet power spectra with NAO. Nevertheless, there is a little coherence between NAO and

either SOI or Niño3 (in spite of their high significance in cross-wavelet power).

[29] The mechanism responsible for the link between the AO and tropical forces is not yet clear, however, for QB signals (2.2–3.5 years) a mechanism has been described by *Baldwin et al.* [2001]: the QBO modulates extra-tropical wave propagation, affecting breakdown of the wintertime stratospheric polar vortices. The polar vortex in the stratosphere affects surface weather patterns providing a mechanism for the QBO to have an effect on high-latitude weather patterns, and hence winter ice severity.

[30] The influence on short timescales of the tropics on the Arctic/North Atlantic area climate has been demonstrated in a number of studies. Results obtained from atmospheric GCMs indicate that the observed trend the AO can be explained as a forced response to the slow changes in world-wide SST, especially the warming of tropical oceans [*Hoerling and Hurrell*, 2001]. *Baldwin and Dunkerton* [2001] show that large anomalies in the stratospheric circulation can influence tropospheric weather patterns in ways analogous to the AO pattern, with delays of 10–60 days between stratosphere and surface. In general tropospheric
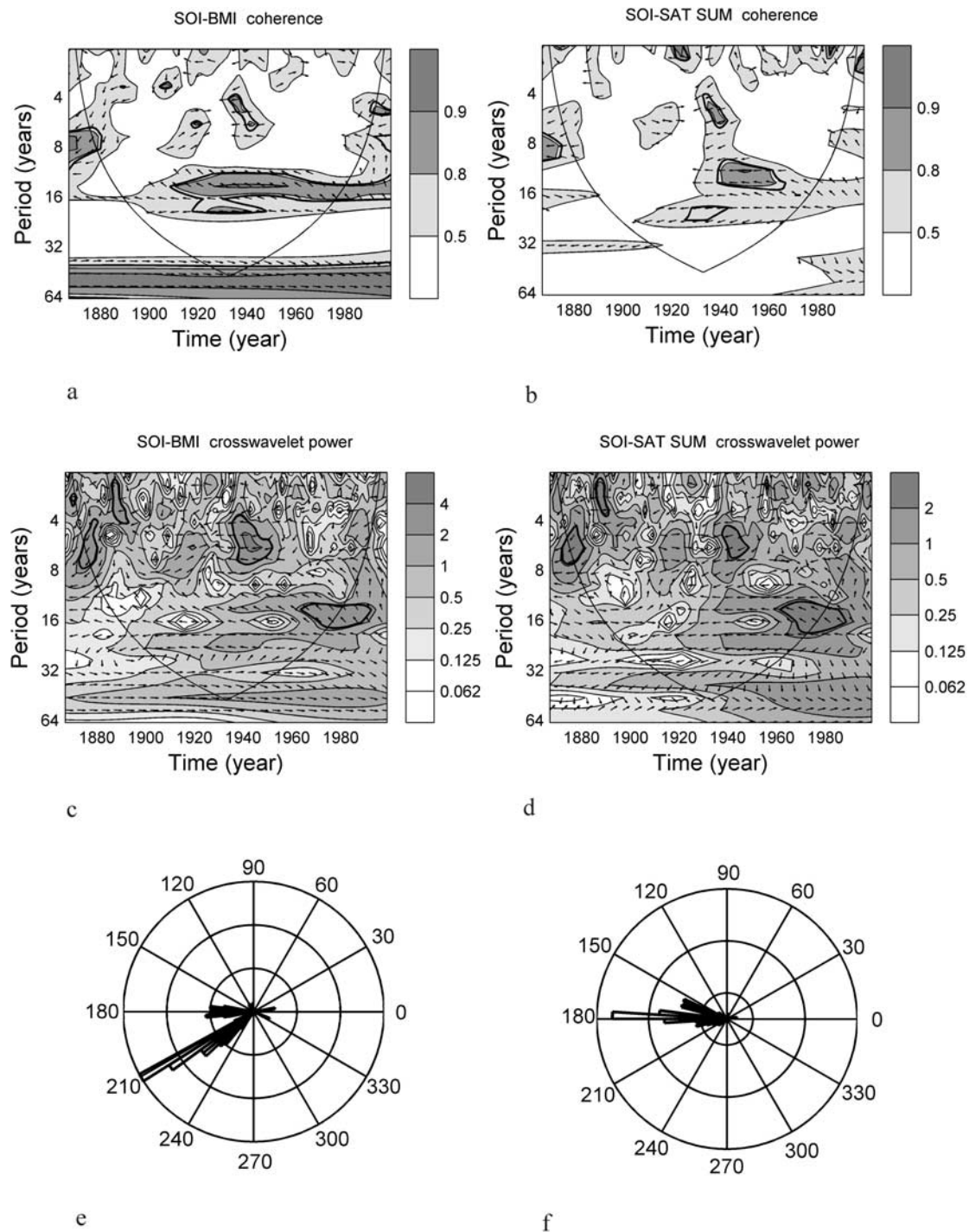
Figure 6. (a) The wavelet coherency and phase between SOI and BMI. Contours are wavelet squared coherencies. The vectors indicate the phase difference between the SOI and BMI. (b) The same as Figure 6a for SOI and sum of negative degree days at Riga (SAT SUM). (c) The cross-wavelet power between SOI and BMI. Contours are for variance units; vectors indicate the phase difference between the SOI/BMI. (d) The same as Figure 6c but for SOI/SAT SUM. (e) SOI/BMI phase angle distribution. (f) SOI/SAT SUM phase angle distribution. In Figures 6a−6d the thick solid line is the 5% significance level using the red noise model, and the thin solid line indicates the cone of influence.

conditions are much more likely to influence stratospheric conditions via angular momentum transferred by upward propagating waves. Several studies [*Glantz et al.*, 1991; *Fraedrich and Müller*, 1992; *Fraedrich*, 1994; *Trenberth et al.*, 1998; *Huang et al.*, 1998; *Dong et al.*, 2000; *Merkel and Latif*, 2002] show that the basic pattern of atmospheric anomalies in the Northern Atlantic sector is forced by SST anomalies outside the Atlantic basin via teleconnections. Recently published results by *Rodwell et al.* [1999], *Mehta et al.* [2000], and *Latif et al.* [2000] argue that the NAO variability is partly forced by global SST and sea ice anomalies. *Hoerling et al.* [2001] show how tropical oceans influence the NAO, however it seems more natural to see the influence as being on AO, which is also reflected in NAO [*Hoerling and Hurrell*, 2001]. The response of the circulation in the North Atlantic region is a mixture of tropical Atlantic forcing related to the tropical Pacific SST anomalies and the midlatitudes atmospheric forcing through the Pacific North American teleconnection over North America. The atmospheric pressure perturbation can be propagated downstream, to other longitudes in the form of Rossby waves, eventually affecting locations far away from the Pacific, particularly the North Atlantic region, with a lag of around three months [*Pozo-Vázquez et al.*, 2001]. This is consistent with our observation that correlations between the AO and SOI/Niño3 indices are best when AO is delayed by 3 months relative to the tropical indices.

[31] The question remains of how tropical signatures with very long (decadal) length periods can be reflected in the AO (or NAO). It seems likely that longer period linkages are mediated by oceanic and/or Arctic Ocean sea ice mechanisms [*Wanner et al.*, 2001]. For example, *Chang et al.* [1997] propose that the position of the inter tropical convergence zone in the tropical Atlantic is related to cross-equatorial SST differences. *Rajagopalan et al.* [1998] shows strong broadband coherence between the NAO and the tropical Atlantic SST in the $8-20$ year period band, suggesting a significant midlatitude-tropical interaction.

[32] Thermohaline circulation changes have also been proposed to explain the long periodicities ($30-60$ years) observed in Atlantic SST anomalies, however the periods seem to be longer than those we observe to be coherent between AO and SOI, which are limited (partly by the length of the records) to about 15 year periods. *Mysak and Venegas* [1998] propose a cycle of roughly decadal length involving sea ice anomalies in the Greenland and Beaufort Seas and sea level pressure (SLP). However, while the frequency of their cycle is similar to the 13-year period we observe in Figure 3, their sea ice data set was only 40 years long. In a more recent analysis of a 90 year sea ice record of rather heterogeneous quality, *Venegas and Mysak* [2000] show that there are several prominent modes of variation in Arctic sea ice, $6-7$ years, $9-10$ years, $16-20$ and $30-50$ years. The $9-10$ year band stands out in winter.

[33] In summary, it appears that some kind of Arctic Ocean sea ice - SLP feedback is the best explanation for the decadal scale links we observe between ENSO/AO and Baltic Sea ice conditions. *Gloersen* [1995] notes that the Arctic ENSO signal (visible in his 9-year satellite sea record only up to the quasi-quadrennial band), leads the SOI signal by several months. However we find that the best relationships between Arctic and ENSO signals

are when ENSO time series are 3 months ahead of the Arctic time series. Using this delay, it is very striking that all the phase relationships we find between ice conditions and ENSO tend to be very close to perfectly in-phase or antiphase, irrespective of the periods of the various cycles found. This suggests that a very fast linkage exists between the tropics and the Arctic that must consequently be via the atmosphere.

6. Conclusions

[34] We have introduced new results from cross-wavelet and coherence analysis between the time series of ice conditions in the Baltic Sea and the atmospheric circulation patterns represented by the NAO and the AO winter index. We provide methods of improving the assessment of statistical significance and confidence intervals of cross-wavelet power and wavelet coherence phase using red noise models and the application of a normalization technique to time series. In conjunction with the independent MC-SSA analysis, the methods provide a remarkable increase in the ability to separate signals from noise. Decomposition of time series locally in both frequency and time provide us with a new view of the rather complicated ice condition variability. Nonlinear interaction cannot be extracted by correlation analysis, and the understanding of the sea ice conditions variability may well require nonlinear analysis methods to elucidate, however we may be given hints from the strength of signals in the tropical and Arctic indices.

[35] In general, results confirm the major influence of the AO on the ice conditions in the Baltic Sea. The signatures of the $2.2-2.8$, 3.5, 5.7, 7.8 and $12-20$ year oscillations associated with SOI and Niño3 SST variability are clearly seen, and confirmed by cross-wavelet power and coherence significance testing against red noise models.

[36] Our results show that highest variability in ice conditions in the Baltic Sea seems to be determined by the influence of the AO via signals of $2.2-7.8$ and $12-20$ year periodicity linked to the events in the tropical Pacific Ocean where signals with the same frequency are generated about three months earlier. The mechanism of linking the tropical signals and the AO and Baltic ice conditions is still rather uncertain. It is likely that the shorter period variations are transmitted via the stratosphere, while the longer periods are most likely characteristic of feedback mechanisms between the SLP fields, sea ice concentration and ocean circulation in the Arctic and sub-Arctic gyre systems.

References

Allen, M. R., and L. A. Smith, Monte Carlo SSA, detecting irregular oscillations in the presence of coloured noise, *J. Clim.*, *9*, 3383–3404, 1996.

Ambaum, M. H. P., B. Hoskins, and D. B. Stephenson, Arctic oscillation or North Atlantic oscillation?, *J. Clim.*, *14*, 3495–3507, 2001.

Baldwin, M. P., and T. J. Dunkerton, Stratospheric harbingers of anomalous weather regimes, *Science*, *294*, 581–584, 2001.

Baldwin, M. P., et al., The Quasi-Biennial Oscillation, *Rev. Geophys.*, *39*, 170–229, 2001.

Bergström, H., and A. Moberg, Daily air temperature and pressure series for Uppsala (1722–1998), *Clim. Change*, *53*, 213–252, 2002.

Cassou, C., and L. Terray, Ocean forcing of the wintertime low-frequency atmospheric variability in the North Atlantic European sector: A study with the ARPEGE model, *J. Clim.*, *14*, 4266–4291, 2001.

Chang, P., L. Ji, and H. Li, A decadal climate variation in the tropical Atlantic Ocean from thermodynamic air-sea interactions, *Nature*, *385*, 516–518, 1997.

Chen, D., and C. Heliström, The influence of the North Atlantic Oscillation on the regional temperature variability in Sweden: Spatial and temporal variations, *Tellus, Ser. A*, *51*, 505–516, 1999.

Deser, C., On the teleconnectivity of the "Arctic Oscillation," *Geophys. Res. Lett.*, *27*, 779–782, 2000.

Dong, B.-W., R. T. Sutton, S. P. Jewson, A. O'Neil, and J. M. Slingo, Predictable winter climate in the North Atlantic sector during the 1997–1999 ENSO cycle, *Geophys. Res. Lett.*, *27*, 985–988, 2000.

Foufoula-Georgiou, E., and P. Kumar (Eds.), *Wavelets in Geophysics*, 373 pp., Academic, San Diego, Calif., 1995.

Fraedrich, K., An ENSO impact on Europe?, *Tellus, Ser. A*, *46*, 541–552, 1994.

Fraedrich, K., and K. Müller, Climate anomalies in Europe associated with ENSO extremes, *Int. J. Climatol.*, *12*, 25–31, 1992.

Glantz, M. H., R. W. Katz, and N. Nicholls, *Teleconnection Linking World Wide Climate Anomalies*, Cambridge Univ. Press, New York, 1991.

Gloersen, R., Modulation of hemispheric sea-ice cover by ENSO events, *Nature*, *373*, 503–505, 1995.

Hoerling, M. P., and J. W. Hurrell, Dynamical forcing of the annular mode and its recent upward trend, *Eos Trans. AGU*, *82*(47), Fall Meet. Suppl., Abstract A31A-09, 2001.

Hoerling, M. P., J. W. Hurrell, and T. Xu, Tropical origins for recent North Atlantic climate change, *Science*, *292*, 90–92, 2001.

Holschneider, M., *Wavelets: An Analysis Tool*, 455 pp., Oxford Univ. Press, New York, 1995.

Huang, J., K. Higuchi, and A. Shabbar, The relationship between the North Atlantic Oscillation and the El Niño-Southern Oscillation, *Geophys. Res. Lett.*, *25*, 2707–2710, 1998.

Hurrell, J. W., Decadal trends in the North Atlantic Oscillation: Regional temperatures and precipitation, *Science*, *269*, 676–679, 1995.

Jevrejeva, S., Severity of winter seasons in the northern baltic Sea during 1529–1990: Reconstruction and analysis, *Clim. Res.*, *17*, 55–62, 2001.

Jevrejeva, S., Association between the ice conditions in the Baltic Sea and the North Atlantic Oscillation, *Nord. Hydrol.*, *33*, 319–330, 2002.

Jevrejeva, S., and J. C. Moore, Singular spectrum analysis of Baltic Sea ice conditions and large-scale atmospheric patterns since 1708, *Geophys. Res. Lett.*, *28*, 4503–4507, 2001.

Jones, P. D., and D. H. Lister, The daily air temperature record for St. Petersburg (1743–1996), *Clim. Change*, *53*, 253–267, 2002.

Jones, P. D., T. Jonsson, and D. Wheeler, Extension using early instrumental pressure observations from Gibraltar and SW Iceland to the North Atlantic Oscillation, *Int. J. Climatol.*, *17*, 1433–1450, 1997.

Kaplan, A., M. A. Cane, Y. Kushnir, A. C. Clement, M. B. Blumenthal, and B. Rajagopalan, Analyses of global sea surface temperature 1856–1991, *J. Geophys. Res.*, *103*, 18,567–18,589, 1998.

Koslowski, G., and R. Glaser, Reconstruction of the ice winter severity since 1701 in the western Baltic, *Clim. Change*, *31*, 79–98, 1995.

Koslowski, G., and R. Glaser, Variations in reconstructed ice winter severity in the western Baltic from 1501 to 1995, and their implications for the North Atlantic Oscillation, *Clim. Change*, *41*, 175–191, 1999.

Latif, M., K. Arpe, and E. Roeckner, Oceanic control of decadal North Atlantic sea level pressure, *Geophys. Res. Lett.*, *27*, 727–730, 2000.

Leppäranta, M., and A. Seinä, Freezing, maximum annual ice thickness and breakup of ice on the Finnish coast during 1830–1984, *Geophysica*, *21*(2), 87–104, 1985.

Lin, H., J. Derome, R. J. Greatbath, K. A. Peterson, and J. Lu, Tropical links of the Arctic Oscillation, *Geophys. Res. Lett.*, *29*(20), 1943, doi:10.1029/2002GL015822, 2002.

Loewe, P., and G. Koslowski, The western Baltic Sea ice season in terms of a mass-related severity index 1879–1992, II Spectral characteristics and associations with NAO, QBO and solar cycle, *Tellus, Ser. A*, *50*, 219–241, 1998.

Mak, M., Orthogonal wavelet analysis: Interannual variability in the sea surface temperature, *Bull. Am. Meteorol. Soc.*, *76*, 2179–2186, 1995.

Mehta, V. M., M. J. Suarez, J. Manganello, and T. L. Delworth, Oceanic influence of the North Atlantic Oscillation and associated Northern Hemisphere climate variations: 1959–1993, *Geophys. Res. Lett.*, *27*, 121–124, 2000.

Merkel, U., and M. Latif, A high resolution AGCM study of the El Niño impact on the North Atlantic/European sector, *Geophys. Res. Lett.*, *29*(9), 1291, doi:10.1029/2001GL013726, 2002.

Meyers, S. D., B. G. Kelly, and J. J. O'Brian, An introduction to wavelet analysis in oceanography and meteorology: With application to the dispersion of Yanai waves, *Mon. Weather Rev.*, *121*, 2858–2866, 1993.

Moberg, A., H. Bergström, J. Ruiz Krigsman, and O. Svanered, Daily air temperature and pressure series for Stockholm (1756–1998), *Clim. Change*, *53*, 171–212, 2002.

Moritz, R. E., C. M. Bitz, and E. J. Steig, Dynamics of recent climate change in the Arctic, *Science*, *297*, 1497–1502, 2002.

Moron, V., R. Vautard, and M. Ghil, Trends, interdecadal and interannual oscillations in global sea-surface temperatures, *Clim. Dyn.*, *14*, 545–569, 1998.

Mysak, L. A., and S. A. Venegas, Decadal climate oscillations in the Arctic: A new feedback loop for atmosphere-ice-ocean interactions, *Geophys. Res. Lett.*, *25*, 3607–3610, 1998.

Omstedt, A., and D. Chen, Influence of atmospheric circulation on the maximum ice extent in the Baltic Sea, *J. Geophys. Res.*, *106*, 4493–4500, 2001.

Pozo-Vázquez, D., M. J. Esteban-Parra, F. S. Rodrigo, and Y. Castro-Diez, The association between ENSO and winter atmospheric circulation and temperature in the North Atlantic Region, *J. Clim.*, *14*, 3408–3420, 2001.

Rajagopalan, B., Y. Kushnir, and Y. M. Tourre, Observed decadal midlatitude and tropical Atlantic climate variability, *Geophys. Res. Lett.*, *25*, 3967–3970, 1998.

Rodwell, M. J., D. P. Rowell, and C. K. Folland, Oceanic forcing of the wintertime North Atlantic Oscillation and European climate, *Nature*, *398*, 320–323, 1999.

Ropelewski, C. F., and P. D. Jones, An extension of the Tahiti-Darwin Southern Oscillation Index, *Mon. Weather Rev.*, *115*, 2161–2165, 1987.

Seinä, A., and E. Palosuo, The classification of the maximum annual extent of ice cover in the Baltic Sea 1720–1995, *Meri Rep. Ser. Finn. Inst. Mar. Res. 27*, Finn. Inst. of Mar. Res., Helsinki, 1996.

Seinä, A., H. Grönvall, S. Kalliosaari, and J. Vainio, Ice seasons 1996–2000 in Finnish sea areas/Jäätalvet 1996–2000 Suomen merialueilla, *Meri Rep. Ser. Finn. Inst. Mar. Res. 43*, Finn. Inst. of Mar. Res., Helsinki, 2001.

Thompson, D. W. J., and J. M. Wallace, The Arctic Oscillation signature in the winter geopotential height and temperature fields, *Geophys. Res. Lett.*, *25*, 1297–1300, 1998.

Torrence, C., and G. P. Compo, A practical guide to wavelet analysis, *Bull. Am. Meteorol. Soc.*, *79*, 61–78, 1998.

Torrence, C., and P. Webster, Interdecadal changes in the ESNO-monsoon system, *J. Clim.*, *12*, 2679–2690, 1999.

Trenberth, K. E., The definition of El Niño, *Bull. Am. Meteorol. Soc.*, *78*, 2771–2777, 1997.

Trenberth, K. E., and J. W. Hurrell, Decadal atmospheric-ocean variations in the Pacific, *Clim. Dyn.*, *9*, 303–309, 1994.

Trenberth, K. E., G. W. Branstator, D. Karoly, A. Kumar, and C. Ropelewski, Progress during TOGA in understanding and modeling global teleconnections associated with tropical sea surface temperatures, *J. Geophys. Res.*, *103*, 14,310–14,324, 1998.

Venegas, S. A., and L. A. Mysak, Is there a dominant timescale of natural climate variability in the Arctic?, *J. Clim.*, *13*, 3412–3434, 2000.

Wallace, J. M., North Atlantic Oscillation/annular mode: Two paradigms—One phenomenon, *Q. J. R. Meteorol. Soc.*, *126*, 791–805, 2000.

Wanner, H., S. Bronnimann, C. Casty, D. Gyalistras, J. Luterbacher, C. Schmutz, D. B. Stephenson, and E. Xoplaki, North Atlantic oscillation-concepts and studies, *Surv. Geophys.*, *22*, 321–382, 2001.

Yiou, P., D. Sornette, and M. Ghil, Data-adaptive wavelets and multi-scale SSA, *Physica D*, *142*, 254–290, 2000.

Zar, J. H., *Biostatistical Analysis*, Prentice-Hall, Old Tappan, N. J., 1999.

———————————

A. Grinsted and J. C. Moore, Arctic Centre, University of Lapland, 96300 Rovaniemi, Finland.

S. Jevrejeva, Proudman Oceanographic Laboratory, Birkenhead CH43 7RA, UK. (sveta@pol.ac.uk)